Taylor & Francis
Taylor & Francis Group

EXTRA VIEW

Identification of proteins associated with splicing factors Ntr1, Ntr2, Brr2 and Gpl1 in the fission yeast *Schizosaccharomyces pombe*

Ingrid Cipakova[a], Matus Jurcik[a], Veronika Rubintova[a], Marianna Borbova[a], Barbora Mikolaskova[a], Jan Jurcik[a], Jana Bellova[b], Peter Barath [b], Juraj Gregan [c,d], and Lubos Cipak [a]

[a]Cancer Research Institute, Biomedical Research Center, University Science Park for Biomedicine, Slovak Academy of Sciences, Bratislava, Slovakia; [b]Institute of Chemistry, Slovak Academy of Sciences, Bratislava, Slovakia; [c]Advanced Microscopy Facility, VBCF and Department of Chromosome Biology, MFPL, University of Vienna, Vienna Biocenter (VBC), Vienna, Austria; [d]Department of Genetics, Faculty of Natural Sciences, Comenius University in Bratislava, Bratislava, Slovakia

ABSTRACT

The spliceosome is a complex molecular machine assembled from many components, which catalyzes the removal of introns from mRNA precursors. Our previous study revealed that the Nrl1 (NRDE-2 like 1) protein associates with spliceosome proteins and regulates pre-mRNA splicing and homologous recombination-dependent R-loop formation in the fission yeast *Schizosaccharomyces pombe*. Here, we identify proteins associated with splicing factors Ntr1, Ntr2, Brr2 and Gpl1, a poorly characterized G-patch domain-containing protein required for efficient splicing. This work provides new evidence that Nrl1 and splicing factors physically interact and reveals additional insights into the protein interaction network of the spliceosome. We discuss implications of these findings in the light of recent progress in our understanding of how Nrl1 and splicing factors ensure genome stability.

Introduction

Splicing of precursor messenger RNA is catalyzed by the spliceosome, which is assembled from many components around a pre-mRNA substrate. The major components of the spliceosome include small nuclear ribonucleoprotein particles containing U1, U2, U4, U5 or U6 snRNA (snRNPs), the nineteen complex (NTC) and the nineteen-related complex (NTR). In addition, there are several other enzymes and cofactors associated with the spliceosome. Recent structural studies together with previous genetic and biochemical analyses provided important insights into the mechanisms of spliceosome assembly and disassembly as well as activation and catalytic reactions. These studies revealed that the spliceosome shows a remarkable structural and mechanistic conservation between yeast and human systems suggesting that the underlying mechanism is conserved across most eukaryotes [1,2].

Previous studies identified Nrl1, a protein sharing similarities with NRDE-2 proteins, as a spliceosome-associated protein that affects mRNA splicing of a subset of genes and non-coding RNAs. Nrl1 also suppresses homologous recombination-dependent R-loop formation and targets transcripts with cryptic introns to form heterochromatin domains at developmental genes and retrotransposons in the fission yeast *Schizosaccharomyces pombe* [3,4]. In this Extra View, we provide an analysis of the spliceosome complex and validate the specificity of interactions between Nrl1 and spliceosome by purifying TAP-tagged splicing factors Ntr1, Ntr2, Brr2 and SPAC20H4.06c, a G-patch domain-containing protein orthologous to human GPATCH1 protein, which we named Gpl1 (*GPATCH1 like 1*) [5,6]. We also discuss insights into the protein interaction network of splicing factors including a possible functional interaction between G-patch domain-containing protein Gpl1 and putative RNA helicase SPAC20H4.09.

Results and discussion

In our previous study, we used tandem affinity purification (TAP) protocol followed by mass-spectrometry analysis to identify proteins associated

---

with Nrl1. We found that splicing factors Ntr1, Ntr2, Brr2 and Gpl1, a poorly characterized G-patch domain-containing protein required for efficient splicing, as well as several other proteins co-purified with Nrl1-TAP [3]. An independent study found that Ntr2 and Gpl1 as well as other splicing factors co-purified with Nrl1-MYC and Nrl1-FLAG [4]. Moreover, we observed an interaction between Nrl1 and Ntr2 in a yeast two-hybrid assay [3].

In order to validate the specificity of interactions between Nrl1 and spliceosomal factors, we decided to perform reciprocal purifications using TAP-tagged Ntr1, Ntr2, Brr2 and Gpl1. We constructed strains expressing TAP-tagged Ntr1 (Ntr1-TAP), Ntr2 (Ntr2-TAP), Brr2 (Brr2-TAP) and Gpl1 (Gpl1-TAP), according to our protocol described at http://mendel.imp.ac.at/Pombe_tagging/ [7]. While *ntr1, ntr2* and *brr2* genes are essential for cell growth [8,9], haploid cells expressing Ntr1-TAP, Ntr2-TAP or Brr2-TAP were viable (data not shown). We used

a TAP protocol to purify Ntr1-TAP, Ntr2-TAP, Brr2-TAP and Gpl1-TAP from cycling *S. pombe* cells and identified co-purifying proteins by mass spectrometry (Figure 1(a,b)). Indeed, we found that Nrl1 co-purified with Ntr11-TAP, Ntr2-TAP, Brr2-TAP as well as Gpl1-TAP (Figure 1(c), Table S1). In addition to Nrl1, we identified many of the known components of the spliceosome with high scores in our purifications (Figure 1(c), Table S1), suggesting that our purifications were specific and many important interactions were preserved.

While many splicing factors such as the Brr2 helicase have been studied in great detail, other proteins involved in splicing are poorly characterized. Gpl1 is a G-patch domain-containing protein required for efficient splicing, but its molecular function is not known [10]. G-patch domain has a characteristic glycine-rich sequence signature, and it is present in many eukaryotic proteins involved in RNA-processing [11]. Previous studies
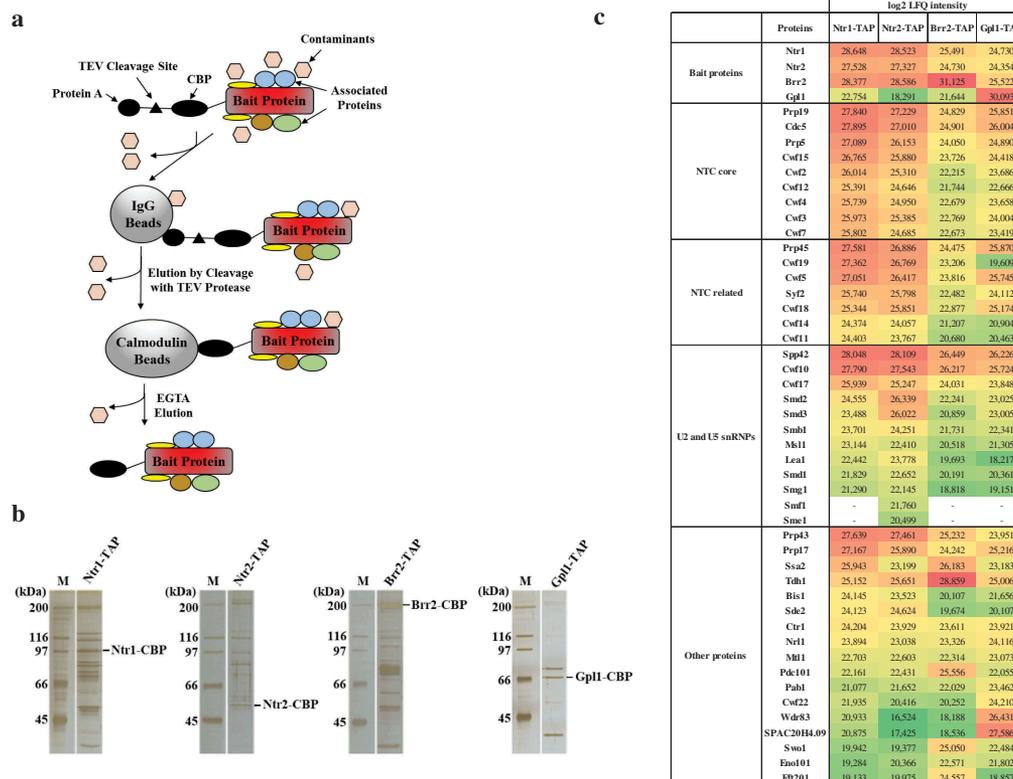
Figure 1. Identification of proteins co-purifying with *S. pombe* Ntr1-TAP, Ntr2-TAP, Brr2-TAP and Gpl1-TAP.
(a) A schematic diagram of the purification protocol. (b) Proteins associated with Ntr1-TAP, Ntr2-TAP, Brr2-TAP and Gpl1-TAP were isolated from cycling *S. pombe* by tandem affinity purification, separated by SDS-PAGE and visualized by silver staining. Molecular weight marker (M) is indicated on the left. (c) List of selected proteins co-purifying with *S. pombe* Ntr1-TAP, Ntr2-TAP, Brr2-TAP and Gpl1-TAP identified by mass spectrometry. For a full list of identified proteins, see Table S1.

		log2 LFQ intensity			
	Proteins	Ntr1-TAP	Ntr2-TAP	Brr2-TAP	Gpl1-TAP
Bait proteins	Ntr1	28,648	28,523	25,491	24,730
	Ntr2	27,528	27,327	24,730	24,354
	Brr2	28,377	28,586	31,125	25,522
	Gpl1	22,754	18,291	21,644	30,093
NTC core	Prp19	27,840	27,229	24,829	25,851
	Cdc5	27,895	27,010	24,901	26,004
	Prp5	27,089	26,153	24,050	24,890
	Cwf15	26,765	25,880	23,726	24,418
	Cwf2	26,014	25,310	22,215	23,686
	Cwf12	25,391	24,646	21,744	22,666
	Cwf4	25,739	24,950	22,679	23,658
	Cwf3	25,973	25,385	22,769	24,004
	Cwf7	25,802	24,685	22,673	23,419
NTC related	Prp45	27,581	26,886	24,475	25,870
	Cwf19	27,362	26,769	23,206	19,609
	Cwf5	27,051	26,417	23,816	25,745
	Syf2	25,740	25,798	22,482	24,112
	Cwf18	25,344	25,851	22,877	25,174
	Cwf14	24,374	24,057	21,207	20,904
	Cwf11	24,403	23,767	20,680	20,463
U2 and U5 snRNPs	Spp42	28,048	28,109	26,449	26,226
	Cwf10	27,790	27,543	26,217	25,724
	Cwf17	25,939	25,247	24,031	23,848
	Smd2	24,555	26,339	22,241	23,025
	Smd3	23,488	26,022	20,859	23,005
	Smb1	23,701	24,251	21,731	22,341
	Msl1	23,144	22,410	20,518	21,305
	Lea1	22,442	23,778	19,693	18,217
	Smd1	21,829	22,652	20,191	20,361
	Smg1	21,290	22,145	18,818	19,151
	Smf1	-	21,760	-	-
	Sme1	-	20,499	-	-
Other proteins	Prp43	27,639	27,461	25,232	23,951
	Prp17	27,167	25,890	24,242	25,216
	Ssa2	25,943	23,199	26,183	23,183
	Tdh1	25,152	25,651	28,859	25,006
	Bis1	24,145	23,523	20,107	21,656
	Sde2	24,123	24,624	19,674	20,107
	Ctr1	24,204	23,929	23,611	23,921
	Nrl1	23,894	23,038	23,326	24,116
	Mtl1	22,703	22,603	22,314	23,073
	Pdc101	22,161	22,431	25,556	22,055
	Pab1	21,077	21,652	22,029	23,462
	Cwf22	21,935	20,416	20,252	24,210
	Wdr83	20,933	16,524	18,188	26,431
	SPAC20H4.09	20,875	17,425	18,536	27,586
	Swo1	19,942	19,377	25,050	22,484
	Eno101	19,284	20,366	22,571	21,802
	Eft201	19,133	19,975	24,557	18,857

showed that G-patch domain proteins contribute to the function of RNA helicases involved in RNA processing [10,12,13]. Interestingly, we found that Gpl1-TAP co-purified with SPAC20H4.09 (Figure 1(c), Table S1), an uncharacterized RNA helicase that shares similarities with human DHX35 [14]. Previous observations that both Gpl1 and SPAC20H4.09 co-purify with splicing factors [15–17] and that *SPAC20H4.09Δ* mutant shows genetic interactions with mutants defective in splicing [18] are consistent with the possible role of SPAC20H4.09 in RNA splicing. *SPAC20H4.09* and *gpl1* genes are located on the same chromosome, separated by only about 4000 bp, suggesting possible common regulation of their expression [14]. Therefore, we speculate that the splicing defect observed in *gpl1Δ* mutant cells might be due to impaired function of the SPAC20H4.09 helicase. Further functional studies of the SPAC20H4.09 helicase and its possible regulation by the G-patch protein Gpl1 are needed to understand their roles in RNA splicing.

Taken together, we show that Nrl1 co-purifies with Ntr1-TAP, Ntr2-TAP, Brr2-TAP and Gpl1-TAP, confirming our previous observation that Nrl1 interacts with splicing factors. In addition, our results provide new insights into the protein interaction network of splicing factors. Based on our results, we speculate that a putative RNA helicase SPAC20H4.09 functionally interacts with the G-patch domain-containing protein Gpl1 required for efficient splicing. Further exploration should reveal a better understanding of the functional relationship between proteins identified in our purifications. Given the conserved nature of these proteins, we expect that our work will shed light on the functions of these proteins both in yeast and higher eukaryotes.

Materials and methods

Strains

S. pombe strains expressing either Ntr1-TAP (FY310, *h⁻ leu1-32 ura4-D18 ade6-M216 ntr1-TAP:: KanMX6*), Ntr2-TAP (FY311, *h⁻ leu1-32 ura4-D18 ade6-M216 ntr2-TAP::KanMX6*), Brr2-TAP (FY307, *h⁻ leu1-32 ura4-D18 ade6-M216 brr2-TAP::*

KanMX6) or Gpl1-TAP (FY331, *h⁻ leu1-32 ura4-D18 ade6-M216 gpl1-TAP::KanMX6*) were grown in complete yeast extract medium (5.0 g/l yeast extract, 3.0% glucose, 0.1 g/l L-leucine, 0.1 g/l L-lysine hydrochloride, 0.1 g/l L-histidine, 0.1 g/l uracil and 0.15 g/l adenine sulfate) at 32°C. TAP-tagging was confirmed by PCR and immunoblotting using PAP antibody (rabbit antiperoxidase antibody linked to peroxidase, Dako) at 1:20.000 dilution (2% skim milk in 0.05% PBS-T).

Protein purification

Fifteen-liter cultures of strains expressing TAP-tagged proteins were grown to mid-log phase (OD_{600} ~ 0.8–1.0) and cells were collected by centrifugation. Yeast cell powders (50 g) were made from frozen cell pellets using SPEX SamplePrep 6770 Freezer/Mill cooled by liquid nitrogen. Proteins were extracted using IPP150 buffer (50 mM Tris pH 8.0, 150 mM NaCl, 10% glycerol, 0.1% NP-40, complete protease and phosphatase inhibitors and 1 mM PMSF). Five hundred microliters of IgG Sepharose™ 6 Fast Flow beads per sample (GE Healthcare) was washed with IPP150 buffer, mixed with protein extracts and rotated for 2 h at 4°C. Beads were washed with 20 volumes of IPP150 buffer and with 5 volumes of TEV cleavage buffer (TCB, 10 mM Tris pH 8.0, 150 mM NaCl, 10% glycerol, 0.1% NP-40, 0.5 mM EDTA and 1 mM DTT). Cleavage step was performed in 2 ml of TCB buffer supplemented with 400 Units of Turbo TEV protease (MoBiTec) for 2 h at 16°C. Two milliliters of eluates was supplemented with 6 μl of 1 M $CaCl_2$ and mixed with 6 ml of Calmodulin binding buffer 1 (CBB1, 10 mM Tris pH 8.0, 150 mM NaCl, 10% glycerol, 0.1% NP-40, 1 mM imidazole, 1 mM Mg-Acetate, 2 mM $CaCl_2$ and 10 mM β-mercaptoethanol). One hundred and fifty microliters of Calmodulin Sepharose™ 4B beads per sample (GE Healthcare) was washed with CBB1 buffer, added to a mixture of eluates and CBB1 buffer and incubated for 2 h at 4°C. The beads were washed with 10 volumes of CBB1 and 5 volumes of Calmodulin binding buffer 2 (CBB2, 10 mM Tris pH 8.0, 150 mM NaCl, 1 mM Mg-Acetate, 2 mM $CaCl_2$ and 1 mM β-mercaptoethanol). The proteins were step-eluted using bead volume of elution buffer (EB, 10 mM Tris pH 8.0, 150 mM NaCl, 1 mM Mg-

acetate, 2 mM EGTA and 1 mM β-mercaptoethanol). Eluted proteins were separated on SDS-PAGE and visualized by silver staining. Eluates from peak fractions were submitted for LC-MS/MS analysis.

LC-MS/MS analysis

Samples were reduced in the presence of 10 mM DTT (30 min, 60°C), alkylated by addition of 30 mM iodoacetamide (20 min, RT/in dark) and the alkylation reaction was quenched by additional 10 mM DTT. One microgram of modified sequencing grade trypsin (Promega) was added to the protein mixture, and the samples were incubated overnight at 37°C. The reaction mixture was acidified by addition of 0.5% TFA, the peptides were purified by microtip C18 SPE and dried in the speedVac. For LC-MS analysis, the set of nanotrap column (Acclaim PepMap100 C18, 75 μm x 20 mm, Dionex, CA, USA) and nanoseparation column (Acclaim PepMap C18, 75 μm x 500 mm, Dionex) attached to UltiMate 3000 RSLCnano system (Dionex, CA, USA) were used. The peptides were separated in 1 h gradient from 3% to 43% B with two mobile phases used: 0.1% FA (v/v) (A) and 80% ACN (v/v) with 0.1% FA (B). Spectral datasets were collected by Orbitrap Elite mass spectrometer (ThermoScientific, MA, USA) operating in the data-dependent mode using Top15 strategy for the selection of precursor ions for the HCD fragmentation [19]. Each of the samples was analyzed in two technical replicates. Obtained datasets were processed by MaxQuant (version 1.5.3.30) [20] with built-in Andromeda search engine using carbamidomethylation (C) as permanent modification and oxidation (M), acetylation (N-terminus) and phosphorylation (STY) as variable modifications. The analysis was performed as LFQ experiment using "match between runs" as an advanced parameter [21]. The search was performed against *the S. pombe* protein database (UniProt, downloaded 25. 08. 2016).

Disclosure statement

No potential conflict of interest was reported by the authors.

ORCID

Peter Barath (iD) http://orcid.org/0000-0001-7330-955X
Juraj Gregan (iD) http://orcid.org/0000-0002-2989-8374
Lubos Cipak (iD) http://orcid.org/0000-0001-7897-6001

References

[1] Plaschka C, Newman AJ, Nagai K. Structural basis of nuclear pre-mRNA splicing: lessons from yeast. Cold Spring Harb Perspect Biol. 2019;11:a032391.

[2] Yan C, Wan R, Shi Y. Molecular mechanisms of pre-mRNA splicing through structural biology of the spliceosome. Cold Spring Harb Perspect Biol. 2019;11: a032409.

[3] Aronica L, Kasparek T, Ruchman D, et al. The spliceosome-associated protein Nrl1 suppresses homologous recombination-dependent R-loop formation in fission yeast. Nucleic Acids Res. 2016;44:1703–1717.

[4] Lee NN, Chalamcharla VR, Reyes-Turcu F, et al. Mtr4-like protein coordinates nuclear RNA processing for heterochromatin assembly and for telomere maintenance. Cell. 2013;155:1061–1074.

[5] Absmeier E, Santos KF, Wahl MC. Functions and regulation of the Brr2 RNA helicase during splicing. Cell Cycle. 2016;15:3362–3377.

[6] Fair BJ, Pleiss JA. The power of fission: yeast as a tool for understanding complex splicing. Curr Genet. 2017;63:375–380.

[7] Cipak L, Spirek M, Novatchkova M, et al. An improved strategy for tandem affinity purification-tagging of Schizosaccharomyces pombe genes. Proteomics. 2009;9:4825–4828.

[8] Kim DU, Hayles J, Kim D, et al. Analysis of a genome-wide set of gene deletions in the fission yeast Schizosaccharomyces pombe. Nat Biotechnol. 2010;28:617–623.

[9] Spirek M, Benko Z, Carnecka M, et al. S. pombe genome deletion project: an update. Cell Cycle. 2010;9:2399–2402.

[10] Larson A, Fair BJ, Pleiss JA. Interconnections between RNA-processing pathways revealed by a sequencing-based genetic screen for pre-mRNA splicing mutants in fission yeast. G3 (Bethesda). 2016;6:1513–1523.

[11] Aravind L, Koonin EV. G-patch: a new conserved domain in eukaryotic RNA-processing proteins and type D retroviral polyproteins. Trends Biochem Sci. 1999;24:342–344.

[12] Robert-Paganin J, Halladjian M, Blaud M, et al. Functional link between DEAH/RHA helicase Prp43 activation and ATP base binding. Nucleic Acids Res. 2017;45:1539–1552.

[13] Warkocki Z, Schneider C, Mozaffari-Jovin S, et al. The G-patch protein Spp2 couples the spliceosome-stimulated ATPase activity of the DEAH-box protein Prp2 to catalytic activation of the spliceosome. Genes Dev. 2015;29:94–107.

[14] Lock A, Rutherford K, Harris MA, et al. PomBase 2018: user-driven reimplementation of the fission yeast database provides rapid and intuitive access to diverse, interconnected information. Nucleic Acids Res. 2019;47:D821–D827.

[15] Thakran P, Pandit PA, Datta S, et al. Sde2 is an intron-specific pre-mRNA splicing regulator activated by ubiquitin-like processing. Embo J. 2018;37:89–101.

[16] Ren L, McLean JR, Hazbun TR, et al. Systematic two-hybrid and comparative proteomic analyses reveal novel yeast pre-mRNA splicing factors connected to Prp19. PLoS One. 2011;6:e16719.

[17] Yan C, Hang J, Wan R, et al. Structure of a yeast spliceosome at 3.6-angstrom resolution. Science. 2015;349:1182–1191.

[18] Ryan CJ, Roguev A, Patrick K, et al. Hierarchical modularity and the evolution of genetic interactomes across species. Mol Cell. 2012;46:691–704.

[19] Michalski A, Damoc E, Lange O, et al. Ultra high resolution linear ion trap Orbitrap mass spectrometer (Orbitrap Elite) facilitates top down LC MS/MS and versatile peptide fragmentation modes. Mol Cell Proteomics. 2012;11:O111 013698.

[20] Cox J, Mann M. MaxQuant enables high peptide identification rates, individualized p.p.b.-range mass accuracies and proteome-wide protein quantification. Nat Biotechnol. 2008;26:1367–1372.

[21] Cox J, Hein MY, Luber CA, et al. Accurate proteome-wide label-free quantification by delayed normalization and maximal peptide ratio extraction, termed MaxLFQ. Mol Cell Proteomics. 2014;13:2513–2526.